BIOMASS AND BIOENERGY 70 (2014) 267–272

Available online at www.sciencedirect.com

ScienceDirect

http://www.elsevier.com/locate/biombioe

An investigation on the characteristics of cellulose nanocrystals from *Pennisetum sinese*

Qi-lin Lu [a], Li-rong Tang [a], Siqun Wang [b], Biao Huang [a,*], Yan-dan Chen [a], Xue-rong Chen [a]

[a] College of Material Engineering, Fujian Agriculture and Forestry University, Fuzhou 350002, China
[b] Center for Renewable Carbon, The University of Tennessee, Knoxville, TN 37996-4570, USA

ARTICLE INFO

Article history:
Received 1 November 2013
Received in revised form
28 August 2014
Accepted 14 September 2014
Available online 1 October 2014

Keywords:
Pennisetum sinese
Cellulose nanocrystals
Preparation
Characterization
Characteristics

ABSTRACT

The aim of this study was to explore the utilization of *Pennisetum sinese* as cellulose source for the preparation of cellulose nanocrystals (CNC). The cellulose was extracted from *P. sinese* by chemical treatment and bleaching, and obtained cellulose nanocrystals by acid hydrolysis. Transmission electron microscopy (TEM) showed that CNC were rod-like with the diameter of 20–30 nm and the length of 200–300 nm. Fourier transform infrared (FTIR) showed that chemical treatment removed most of the lignin and hemicellulose from *P. sinese*, and CNC had similar structure to that of native cellulose. The crystallinity indexes calculated from X-ray diffraction (XRD) for *P. sinese* and CNC were 40.6% and 77.3%, respectively. The zeta-potential analysis showed that CNC had higher stability than *P. sinese* had. The thermal stability was investigated by thermogravimetric analysis (TGA), and the result showed that *P. sinese* had higher thermal stability than that of prepared CNC.

© 2014 Elsevier Ltd. All rights reserved.

1. Introduction

Cellulose, the most abundant renewable biomacromolecule available on the earth, is widely used because of its biodegradability, biocompatibility and chemical stability [1]. Green plants developed to produce desired products and energy could be possible in the future [2]. The major source of cellulose is wood. However, with the increasing consumption of wood resources and deforestation, many environmental problems arose, therefore developing alternative sources of wood as the cellulose source is essential. *Pennisetum sinese* is a hybrid of *Pennisetum purpureum* and *Pennisetum americanum*, and it is a monocot C4 perennial grass. It is tall and forms in robust bamboo-like clumps. This species has high biomass production, at about 40 t ha^{-1} y^{-1} and can be harvested 3–4 times per year. *P. sinese* is a versatile and adaptable plant. It can grow and even thrive in many weather conditions, lengths of growing seasons, soil types, and land conditions. The cellulose content of *P. sinese* is approximately 35%–50%, the fiber length is 1.48 mm and the fiber width is 30 μm. Therefore, the utilization of *P. sinese* as the primary source of cellulose is promising.

Cellulose nanocrystals (CNC) are referred to as nanocrystals, nanoparticles, microcrystals, or nanofibers. CNC have special spectral characters and high surface area [3]. Recently, there has been a great deal of research interest in utilizing CNC as reinforcement in composite manufacturing, due to their low density, high strength, remarkable reinforcing capacity and environmental benefits [4].

---

* *Corresponding author*. Tel.: +86 591 88160598; fax: +86 591 83715175.
E-mail address: fjhuangbiao@hotmail.com (B. Huang).

http://dx.doi.org/10.1016/j.biombioe.2014.09.012
0961-9534/© 2014 Elsevier Ltd. All rights reserved.

The main objective of this study was to investigate the viability of *P. sinese* as a renewable and low-cost source of cellulose source and extract cellulose nanocrystals from *P. sinese*. Cellulose, hemicellulose, lignin and ash contents of *P. sinese* were determined by chemical analysis. The morphology of separated CNC was investigated by transmission electron microscopy (TEM). The chemical structural changes were revealed by Fourier transform infrared spectroscopy (FTIR). The crystallinity index and thermal stability were investigated by X-ray diffraction (XRD) and thermogravimetric analysis (TGA), respectively. The electrochemical ability was revealed by zeta-potential analysis.

2. Materials and methods

2.1. *Materials*

P. sinese was supplied by China National Engineering Research Center of JUNCAO Technology (Fuzhou, China). Sodium hydroxide, sodium hypochlorite and sulfuric acid (Sinopharm Chemical Reagent Co., Ltd) were all of analytical grade.

2.2. *Cellulose extraction*

P. sinese was harvested in the field of Fuzhou in China's Fujian Province and the elevation was 600–1000 m (26.08N, 119.3E). The growth of *P. sinese* for two years was selected as the raw material to extract cellulose, and the cellulose was extracted from the stalks of *P. sinese*. We know that during the early years of growth, plant usually has a lower cellulose and a higher lignin content [5]. Therefore, two-year growing period *P. sinese* was selected as the raw material in our experiment. The harvested *P. sinese* in the field was chopped to produce a size-reduced flowable material with forage harvesting equipment, and the processing size-reduced product was transported to the storage site. The size-reduced *P. sinese* was air dried until the mass fraction of water was less than 20%, which was to reduce the risk of detrimental biological activity. The dried sample was placed into polypropylene mesh bags to store. Cellulose was extracted from *P. sinese* by alkaline cooking method with alkaline hydroxide, and bleached with sodium hypochlorite [6]. Before the extraction of cellulose, the dried *P. sinese* was cut into cut into small pieces and then the pieces was milled and screened to select the fraction of particles that were beyond 40–60 mesh. The powders was first disintegrated with sodium hydroxide at 160 °C for 150 min, and the residues were allowed to cool and then washed with distilled water until the PH was up to 7.0. The residues were bleached with sodium hypochlorite for 2.0 h to further delignification. The solids were separated from the liquid phase by filtration and washed sequentially with distilled water to neuter. After the treatments of alkaline hydroxide and sodium hypochlorite, most lignin was removed and the cellulose was obtained. The extracted cellulose was dried and stored in a vacuum dryer as the raw material to prepare cellulose nanocrystals.

2.3. *Manufacture of cellulose nanocrystals*

2.0 g extracted *P. sinese* cellulose was hydrolyzed with 50% sulfuric acid at 65 °C under ultrasonic treatment at 250 W with continuous stirring. After 120 min, the cellulose suspension was diluted with distilled water to stop the hydrolysis and allowed to settle for several hours until the suspension was layered, and the clear top layer was decanted off, and then repeatedly washed with distilled water until it was not layered. CNC suspension was obtained after repeated centrifugations. The neutral upper solution was collected and referred to as CNC colloid. After freeze drying, CNC powders were collected.

2.4. *Chemical analysis*

The chemical composition of *P. sinese* was investigated according to ASTM methods: Holocellulose (ASTM D 1104-56) [7], alpha-Cellulose (ASTM D 1103-60) [8], lignin (ASTM D 1106-56) [9], and ash content (ASTM D 1102-84) [10].

2.5. *Transmission electron microscopy*

Transmission electron microscopy (Hitachi-H7650 TEM) was used to investigate the morphology of CNC. A drop of a diluted sample was deposited on a carbon coated grid and allowed to dry at room temperature. The acceleration voltage was 80 kV.

2.6. *Fourier transform infrared spectroscopy*

Fourier transformation infrared spectroscopy (FTIR) was performed by means of a Nicolet 380 FTIR Spectrometer (Thermo electron Instruments Co., Ltd., USA) in the range of 4000–400 cm^{-1} with a resolution of 4 cm^{-1}. Each sample was grinded into powder and blended with KBr, then was pressed into thin pellet.

2.7. *X-ray analysis*

The crystallinity indexes of *P. sinese*, extracted *P. sinese* cellulose and CNC were determined by X-ray analysis. As for X-ray diffraction (XRD), data were collected with a X'Pert Pro MPD X-ray diffractometer equipped with Cu Kα radiation at wavelength $\lambda = 0.154$ nm. Diffractograms were collected in the range of $2\theta = 6–90°$ with a scanning rate of 0.1° s^{-1}.

2.8. *Thermogravimetric analysis*

The thermal stability of extracted *P. sinese* cellulose and CNC were investigated by means of a thermogravimetric analyzer (NETZSCH STA449F3). All the measurements were performed under a nitrogen atmosphere with a gas flow of 30 cm^3 min^{-1}. Each sample was heated from 25 °C to 500 °C at a rate of 10 K min^{-1}. The amount of sample for each measurement was about 5.0 mg.

2.9. *Zeta-potential analysis*

The electrochemical property of CNC was investigated by zeta-potential analysis. Potential charges on the surface of extracted *P. sinese* cellulose and CNC in pure water were determined with a SZP-06 Zetasizer. Extracted *P. sinese* cellulose and CNC suspension were previously ultrasonic treated for 30 min.

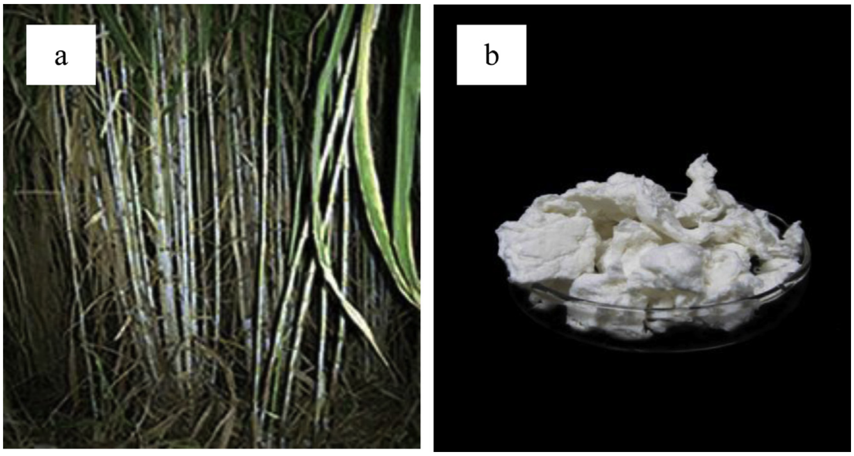

Fig. 1 – **Photographs of (a)** ***Pennisetum sinese*****; (b) extracted cellulose.**

3. Results and discussion

Fig. 1 presents the photographs of *P. sinese* and extracted *P. sinese* cellulose. Visually, white colored cellulose was obtained, indicating that a great part of the initial non-cellulosic components were removed by purification process. Table 1 shows the chemical composition of *P. sinese*. The results show that *P. sinese* enjoys higher mass fraction of cellulose, approximately (45.3 ± 2.2%), the lignin (20.9 ± 2.4%), the hemicellulose (20.5 ± 2.3%) and the ash (3.3 ± 0.3%), which indicates that cellulose is the predominant polysaccharide. The sum of the percentage of cellulose, lignin, hemicellulose and ash to the *P. sinese* corresponds to 90% of the total dry matter, showing that there are other components such as protein and extractives in the *P. sinese*. The alkali treatment can solubilize the lignin, pectins, hemicelluloses and proteins, while the bleaching was applied to remove the lignin residues.

The chemical structure changes among *P. sinese*, extracted *P. sinese* cellulose and CNC were analyzed by FTIR spectroscopy. FTIR spectra of *P. sinese*, extracted *P. sinese* cellulose and CNC are shown in Fig. 2. The broad band at 3408 cm^{-1} corresponds to the stretching of –OH groups and the band at 2901 cm^{-1} corresponds to the C–H stretching of methyl and methylene groups [11]. The band at 1733 cm^{-1} corresponds to the carbonyl groups due to the presence of acetyl ester and carbonyl aldehyde groups of hemicellulose and lignin [12]. This band disappears in the extracted *P. sinese* cellulose and CNC, which demonstrates the most removal of lignin and hemicellulose from *P. sinese* during the alkaline cooking. The bands at 1464 cm^{-1} and 1513 cm^{-1} in *P. sinese* correspond to the C–H deformation in methyl, methylene and methoxyl groups of lignin and aromatic C=C ring stretching [13,14]. These bands disappear in the extracted *P. sinese* cellulose and CNC due to the removal of lignin by bleached treatment with sodium hypochlorite [15]. The band at 1240 cm^{-1} corresponds to the –COO vibration of acetyl groups in hemicellulose [11]. This band disappears in the extracted *P. sinese* cellulose and CNC due to the most removal of hemicellulose during the chemical treatment. The small and sharp band at 895 cm^{-1} corresponds to glycosidic –C_1–H deformation, with ring vibration contribution and –O–H bending vibration, which reveals the typical structure of cellulose [16]. These characters are characteristic of β-glycosidic linkages between the anhydroglucose units in cellulose. FTIR spectra agree with the removal of lignin and hemicellulose during the cellulose extraction. Moreover, the infrared spectra also provide evidence that CNC have similar structure to that of native cellulose.

Table 1 – **The chemical composition of** ***Pennisetum sinese*****.**

Materials	Mass fraction (%)
Cellulose	45.3 ± 2.2
Hemicellulose	20.5 ± 2.3
Lignin	20.9 ± 2.4
Ash	3.3 ± 0.3

The morphology of CNC was studied by means of transmission electron microscopy (TEM). Fig. 3 shows the morphology of CNC. It can be observed that CNC present rod-like shape with a diameter of 20–30 nm and a length of 200–300 nm. The aspect ratio of the rods is high. Cellulose nanocrystals form an interconnected web-like structure.

The X-ray diffractograms of *P. sinese*, extracted *P. sinese* cellulose and CNC are shown in Fig. 4. The diffractogram of *P. sinese* is indicative of a low crystallinity with relatively low

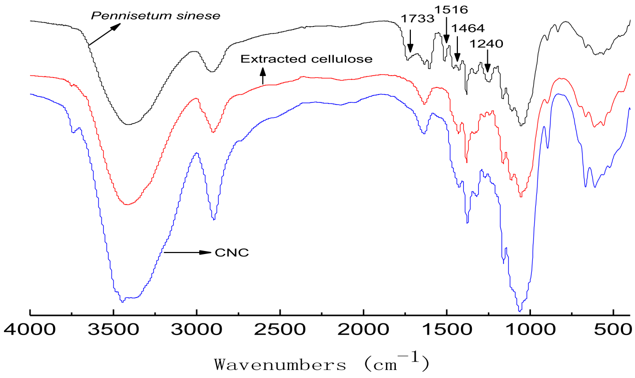

Fig. 2 – **FTIR spectra of** ***Pennisetum sinese*****, extracted cellulose and CNC.**

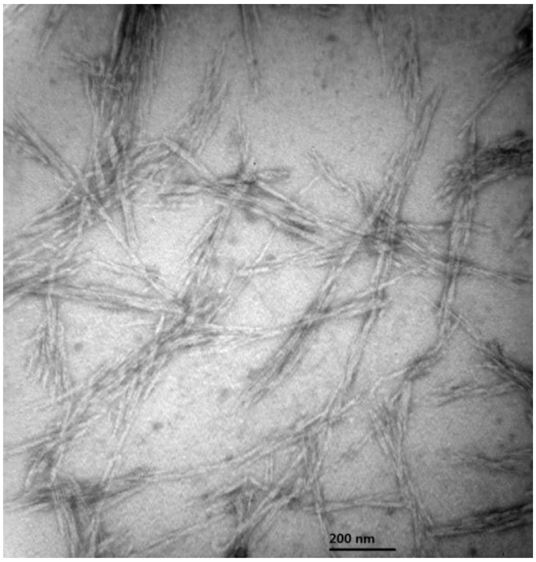

Fig. 3 – Transmission electron microscope of CNC.

intensity peaks at $2\theta = 15.7°$, $22.67°$. Three peaks were observed for the extracted *P. sinese* cellulose and CNC at $2\theta = 15.7°$, $22.67°$ and $34.5°$. These peaks are characteristic of the crystal polymorphs of celluloseI [17]. The crystallinity indexes (CrI) of all samples can be calculated by Segal method [18] as shown in the following Equation:

$$\mathrm{CrI} = \frac{I_{002} - I_{am}}{I_{002}} \times 100$$

where I_{002} is the overall intensity of the peak at 2θ about 22°, representing crystalline material, and I_{am} is the intensity of the baseline at 2θ about 18°, representing amorphous material. The crystallinity indexes of *P. sinese*, extracted *P. sinese* cellulose and CNC are 40.6%, 70.7% and 77.3%, respectively. The increase of crystallinity index from the extracted *P. sinese* cellulose to CNC is due to the acid hydrolysis, leading to the hydrolysis of amorphous regions and promoting the formation of single crystal [19].

Table 2 – Average values of the zeta-potential of the fibres under different conditions.

Samples	Zeta-potential (mv)
Pennisetum sinese fibers	−8
Extracted cellulose fibers	−16.7
CNC (90 min)	−23.8
CNC (120 min)	−28.8
CNC (150 min)	−20

The average values of zeta-potential are shown in Table 2. Higher values of zeta-potential indicate higher capacity of dispersion in water, while low values indicate low dispersion stability. As to *P. sinese* fibers, the capacity of dispersion in water is poor, which can be attributed to the presence of lignin and hemicellulose [20]. CNC present higher zeta-potential values because of sulfuric acid hydrolysis. Sulfuric acid hydrolysis of cellulose induces the grafting of the sulfate groups, randomly distributed on the surface of CNC and leads to the creation of small particles with a large mean surface charge [21]. Due to the effect of electrostatic repulsion between the negatively charged particles, the CNC suspensions that neither precipitate nor flocculate. In a short period of time, the hydrolysis of cellulose could not happen effectively. It is known that insufficient hydrolysis of cellulose may result in large particles (less surface area per unit mass) with a lower mean surface charge, favoring particle–particle interaction and gelation [22]. As expected, increasing the hydrolysis time from 90 min to 120 min led to the increase of surface charges on CNC, consequently, increase the zeta-potential. The increase in hydrolysis time from 120 min to 150 min decreased the zeta-potential values of CNC. It was due to the over-degradation of cellulose. With excess hydrolysis time, cellulose was broken into its component sugar molecules and therefore the zeta-potential values decreased. The zeta-potential values in the present work are similar to previous report for *Eucalyptus* whiskers, which showed that increasing hydrolysis time led to increase of the sulfur content, but decrease of the zeta-potential of the whiskers [23].

Thermal stability of *P. sinese* and CNC were determined by the thermogravimetric method. Fig. 5 shows the thermograms. The degradation onset temperature and corresponding degradation peak position obtained from DTG curves (Fig. 6) are shown in Table 3. As for all the samples, the first mass loss is below 100 °C, corresponding to the vaporization of bound water. As to *P. sinese*, the initial thermal decomposition occurs

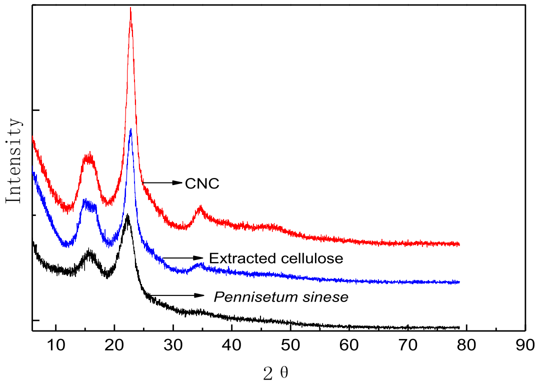

Fig. 4 – X-ray diffraction patterns of *Pennisetum sinese*, extracted cellulose and CNC.

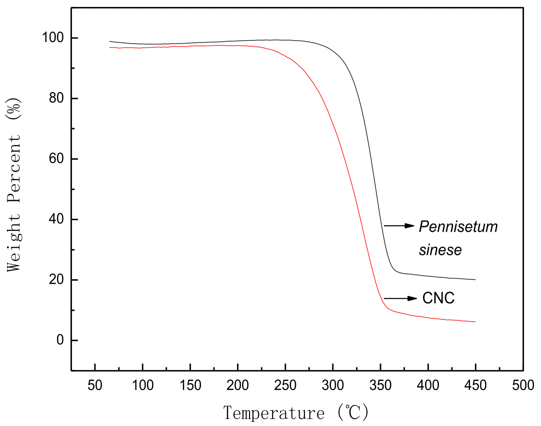

Fig. 5 – Thermograms Of *Pennisetum sinese* and CNC.

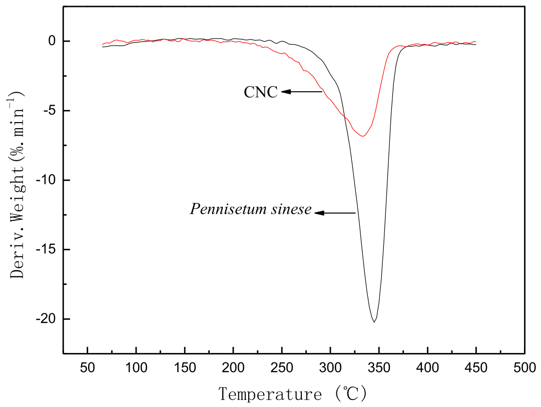

Fig. 6 – DTG curves of *Pennisetum sinese* and CNC.

Table 3 – The degradation onset and peak temperatures of *Pennisetum sinese* and CNC.

Materials	Degradation onset temperature (°C)	Degradation peak temperature (°C)
Pennisetum sinese	257	345
CNC	236	332

at 257 °C until approximately 345 °C, corresponding to the degradation of hemicellulose [24]. The second stage occurs at 345 °C until 450 °C, corresponding to the degradation of cellulose and lignin [25]. At this stage almost all cellulose component is decomposed. As for CNC, the thermal decomposition occurs at 236 °C until approximately 332 °C, indicating typical phenomenon of sulfuric acid-hydrolyzed cellulose nanocrystals [26]. The acid hydrolysis of cellulose introduces sulfate groups on the surface of CNC, leading to lower thermal stability [27]. The study shows that CNC separated from *P. sinese* have lower thermal stability than that of *P. sinese*. It may be due to the harsh chemical treatment of *P. sinese* during the preparation of CNC, which breaks the cellulose chains and decreases the degree of polymerization.

4. Conclusions

This study shows that *P. sinese* could be an excellent cellulose source for the preparation of cellulose nanocrystals. *P. sinese* enjoys higher mass fraction of cellulose, approximately (45.3 ± 2.2%). The characteristics of the prepared cellulose nanocrystals were investigated in the experiment, the results showed that chemical treatment removed most of the lignin and hemicellulose from *P. sinese*, and CNC had similar structure to that of native cellulose. The crystallinity indexes calculated from XRD for *P. sinese* and CNC were 40.6% and 77.3%, respectively.

Acknowledgments

We appreciate the generous financial support of the Project of Advanced Forestry Science and Technology (Grant No. 2014-4-30) and the National Natural Science Foundation of China (Grant No. 31170520, 31370560).

REFERENCES

[1] Zhang JH, Song HN, Lin L, Zhuang JP, Pang CS, Liu SJ. Microfibrillated cellulose from bamboo pulp and its properties. Biomass Bioenergy 2012;39:78–83.
[2] Chum HL, Overend RP. Biomass and renewable fuels. Fuel Process Technol 2001;71(1–3):187–95.
[3] Tang LR, Huang B, Ou W, Chen XR, Chen YD. Manufacture of cellulose nanocrystals by cation exchange resin-catalyzed hydrolysis of cellulose. Bioresour Technol 2011;102(23):10973–7.
[4] Maheswari CU, Reddy KO, Muzenda E, Guduri BR, Rajulu AV. Extraction and characterization of cellulose microfibrils from agricultural residue-*Cocos nucifera* L. Biomass Bioenergy 2012;46:555–63.
[5] Barton, GM. Definition of biomass samples involving wood, bark and foliage. Biomass;4(44):311–14.
[6] Moran JI, Alvarez VA, Cyras VP, Vazquez A. Extraction of cellulose and preparation of nanocellulose from sisal fibers. Cellulose 2008;15(1):149–59.
[7] ASTM D1104-56. Standard test method for holocellulose in wood. Philadelphia PA: American Society for Testing and Materials; 1978.
[8] ASTM D1103-60. Standard test method for alpha-cellulose in wood. Philadelphia PA: American Society for Testing and Materials; 1977.
[9] ASTM D 1106-56. Standard test method for lignin in wood. Philadelphia PA: American Society for Testing and Materials; 1974.
[10] ASTM D 1102-84. Standard test method for ash in wood. Philadelphia PA: American Society for Testing and Materials; 2007.
[11] Reddy KO, Guduri BR, Rajulu AV. Structural characterization and tensile properties of borassus fruit fibers. J Appl Polym Sci 2009;114(1):603–11.
[12] Alemdar A, Sain M. Isolation and characterization of nanofibers from agricultural residues-wheat straw and soy hulls. Bioresour Technol 2008;99(6):1664–71.
[13] Stuart BH. Infrared spectroscopy: fundamentals and applicationsvol. 1. Chichester: John Wiley & Sons; 2004. ISBN 978-0-470-85428-0.
[14] Sain M, Panthapulakkal S. Bioprocess preparation of wheat straw fibers and their characterization. Ind Crop Prod 2006;23(1):1–8.
[15] Xiao B, Sun XF, Sun RC. Chemical, structural, and thermal characterization of alkali-soluble lignins and hemicelluloses, and cellulose from maize stems, rye straw, and rice straw. Polym Degrad Stabil 2001;74(2):307–19.
[16] Alemdar A, Sain M. Biocomposites from wheat straw nanofibers: morphology, thermal and mechanical properties. Compos Sci Technol 2008;68(2):557–65.
[17] Bondeson D, Mathew A, Oksman K. Optimization of the isolation of nanocrystals from microcrystalline cellulose by acid hydrolysis. Cellulose 2006;13(2):171–80.
[18] Segal L, Creely JJ, Martin AE, Conrad CM. An empirical method for estimating the degree of crystallinity of native cellulose using the X-ray diffractometer. Text Res J 1959;29(10):786–94.
[19] Li R, Fei J, Cai YR, Li YF, Feng JQ, Yao JM. Cellulose whiskers extracted from mulberry: a novel biomass production. Carbohydr Polym 2009;76(1):94–9.
[20] Siqueira G, Bras J, Dufresne A. Cellulose whiskers versus microfibrils: influence of the nature of the nanoparticle and

its surface functionalization on the thermal and mechanical properties of nanocomposites. Biomacromolecules 2009;10(2):425–32.

[21] Podsiadlo P, Choi SY, Shim B, Lee J, Cuddihy M, Kotov NA. Molecularly engineered nanocomposites: layer-by-layer assembly of cellulose nanocrystals. Biomacromolecules 2005;6(6):2914–8.

[22] Hebeish A, Guthrie JT. The chemistry and technology of cellulosic copolymers. New York: Springer-Verlag; 1981.

[23] Tonoli GHD, Teixeira EM, Corrêa AC, Marconcini JM, Caixeta LA, Pereira-da-Silva MA, et al. Cellulose micro/nanofibres from *Eucalyptus* kraft pulp: preparation and properties. Carbohydr Polym 2012;89(1):80–8.

[24] Troedec M, Sedan D, Peyratout C, Bonnet JP, Smith A, Guinebretiere R, et al. Influence of various chemical treatments on the composition and structure of hemp fibers. Compos Part A 2008;39(3):514–22.

[25] Prins MJ, Ptasinski KJ, Janssen FJJG. Torrefaction of wood: part 1. Weight loss kinetics. J Anal Appl Pyrol 2006;77(1):28–34.

[26] Roman M, Winter WT. Effect of sulfate groups from sulfuric acid hydrolysis on the thermal degradation behavior of bacterial cellulose. Biomacromolecules 2004;5(5):1671–7.

[27] Wang N, Ding E, Cheng R. Thermal degradation behavior of spherical cellulose nanocrystals with sulfate groups. Polymer 2007;48(12):3486–93.